View metadata, citation and similar papers at core.ac.uk

brought to you by CORE

provided by IntechOpen

We are IntechOpen, the world's leading publisher of Open Access books Built by scientists, for scientists

4,800
Open access books available

122,000
International authors and editors

135M
Downloads

154
Countries delivered to

Our authors are among the

TOP 1%
most cited scientists

12.2%
Contributors from top 500 universities

WEB OF SCIENCE™

Selection of our books indexed in the Book Citation Index in Web of Science™ Core Collection (BKCI)

Interested in publishing with us? Contact book.department@intechopen.com

Numbers displayed above are based on latest data collected.
For more information visit www.intechopen.com

15

Improved Combustion Control in Diesel Engines Through Active Oxygen Concentration Compensation

Jason Meyer and Stephen Yurkovich
The Ohio State University and University of Texas at Dallas
USA

1. Introduction

Like any other chemical reaction, the process of burning fuel depends on the quantities of the reactants involved; for a combustion reaction, those are fuel and oxygen. The unsteady nature of a diesel engine both inside and outside of the cylinders, however, makes the problem of combustion control much more complex than simply regulating the trapped oxygen mass and the fuel injection mass. Because liquid fuel is injected directly into the combustion chamber, several processes must occur before combustion can commence. First, the liquid fuel stream must be atomized. Next, the fuel droplets must be vaporized. Finally, the fuel must mix with the oxygen already residing in the cylinder to form a combustible mixture. Even though the ratio of the total oxygen mass to the total mass of fuel is often significantly lean relative to stoichiometry, the local ratios can be much richer than stoichiometry. As the fuel spray mixes with the trapped charge gases, the local oxygen to fuel ratios at the boundaries of the fuel spray approach stoichiometry and the fuel begins to ignite. Once the combustion process has started, the burn rate is primarily limited by the rate at which the unburned fuel can mix with the remaining oxygen.

Modern diesel engines have sophisticated fuel injection systems that allow for multiple fuel injection pulses, thus providing the ability to flexibility shape the combustion process. The timing of these injections and the fraction of the fuel delivered by each injection strongly affects the combustion process. Injecting fuel prior to the main injection (termed a pilot injection) adds energy and turbulence to the combustion mixture thereby reducing the ignition delay of the main injection, especially at low temperatures (MacMillan et al., 2009; Osuka et al., 1994). This allows for the majority of the heat release to occur when the piston is close to top-dead-center which results in a higher thermodynamic efficiency. However, the improvement in fuel consumption can also be accompanied by an unwanted increase in NO_x emissions (Benajes et al., 2001).

Injecting fuel after the main injection (termed a post injection) adds energy to the system after the primary combustion process has occurred. This energy increases the temperature of the combustion gases at the end of the combustion cycle without increasing the peak combustion temperature, which dictates the production of NO_x. A higher end-of-cycle temperature promotes higher soot oxidation rates and an overall decrease in the engine-out

soot levels (Benajes et al., 2001). Higher end-of-cycle temperatures are also very important to the efficiency of aftertreatment components such as selective catalytic reduction systems.

Controlling a diesel engine is particularly challenging because the evolution of the combustion process depends on numerous factors including: the air charge density, the mass of oxygen gas, the mass of dilutent gases, the mixture homogeneity, the fuel injection mass, the fuel injection timing, the fuel injection pressure and the speed of the engine. Further complicating the control problem, combustion performance is often defined with respect to multiple metrics including torque response, noise, fuel consumption and emissions production. To achieve the best trade-off between these factors, the fueling injection parameters must be precisely matched to the in-cylinder conditions. Typically, a diesel engine is controlled using the type of control structure shown in Figure 1. Such a control system consists of a supervisory controller, a setpoint determination system including a feed-forward fueling controller and an air path controller (Guzzella & Amstutz, 1998). At the highest level, the supervisory controller selects the system operating mode depending on the dynamics of the system (i.e. steady-state versus transient operation), the barometric pressure, the states of the aftertreatment systems (e.g. the soot level within a diesel particulate filter) and other off-nominal considerations (e.g. turbocharger surge prevention).

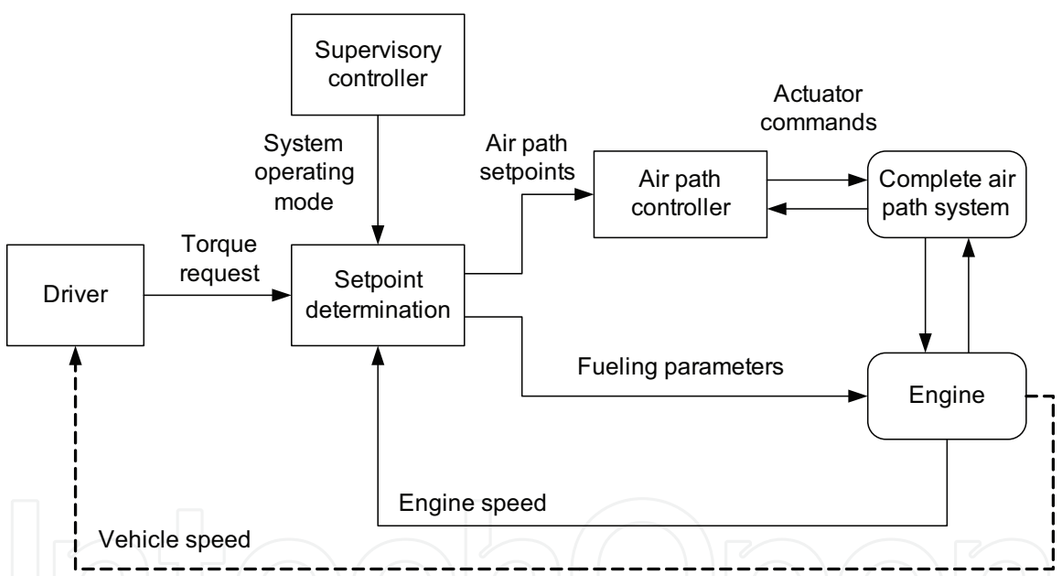

Fig. 1. Current approach to diesel engine control

The setpoint determination system first calculates the mass of fuel required to achieve the driver's torque request. Then based on the system operating mode, the setpoint determination system simultaneously identifies the desired air path response and the desired fuel injection strategy for the current engine speed and calculated fuel mass. Typically, this is achieved using different sets of three-dimensional air path setpoint and fueling parameter setpoint tables. The air path setpoints are passed to an air path controller, whereas the fueling parameters directly drive the fuel injection system. Because of the mass accumulation and mass transport dynamics within the air path system, the response time of a closed loop air path control system is much slower than the response time of a fueling controller. While it may take many engine cycles for an air path controller to change the cylinder contents from one set of desired conditions to another, the fuel delivery method can be arbitrarily changed each injection event.

Selecting the fueling parameters based on the engine speed, desired torque request and system operating mode inherently ignores the dynamics of the air path system. As a result, the injected fuel may combust in a manner which produces less torque, more emission, more noise and/or undesirable engine-out gas temperatures. Additionally, the current method of fueling control lacks robustness. Any variation in the behavior of the air path system can lead to combustion performance degradation.

This chapter develops a new approach to diesel engine fueling control which controls the fuel injections process based on the in-cylinder contents. An integral part of this design is a new air path oxygen dynamics model. By directly predicting the transport delay within the air path system, this model achieves nearly the same accuracy as a one-dimensional model but has the complexity of a zero-dimensional model. The performance of both the delay based oxygen dynamics model and the proposed fueling control structure are demonstrated in simulation.

2. In-cylinder contents based diesel fueling control

Although diesel engine combustion depends on numerous factors, a production diesel engine cannot account for all of them. Firstly, identifying each factor and its exact impact is far too time consuming. Engine calibration processes must be kept as short as possible to minimize both cost and the time to market. Secondly, an engine control unit (ECU) has limited processing power and on-board memory. Lastly, many of the factors that affect combustion such as in-cylinder motion (e.g. swirl and tumble) are extremely difficult to measure or estimate. Rather than predicting each of the factors influencing combustion and optimizing the fuel injection parameters online, the optimal fuel parameters are identified *a priori* and stored in lookup tables.

During the engine calibration process, the fueling parameters and air path setpoints which produce the best trade-off between torque response, noise, fuel consumption and emissions production are established for a wide range of engine operating conditions. In a conventional diesel engine control structure, the air path setpoints and fueling parameters identified as optimal are then fit to sets of three-dimensional tables indexed by engine speed, the fuel injection mass and the system operating mode. The fueling parameters selected by this mapping structure do not directly account for the instantaneous cylinder conditions but rather indirectly account for the nominal set of cylinder conditions that correspond to ideal air path performance. During transients or in the presence of system faults, however, the instantaneous in-cylinder conditions deviate from their nominal values. As a result the typical control structure can significantly misestimate the fueling parameters.

A more robust alternative is to schedule the fueling parameters using a variable which represents the achieved in-cylinder contents rather than the expected conditions. Figure 2 illustrates how such a selection scheme could be integrated into the overall diesel engine control structure. As with a traditional controller, the fueling parameters are still selected based on sets of lookup tables, but in this architecture one of the indexing variables is related to the properties of the cylinder contents. With this structure, the fueling controller is no longer autonomous with respect to the air path system. The interconnection between the fueling controller and the air path system through the cylinder contents predictor significantly improves the robustness of the overall engine control system. It should be noted that the air path setpoints can still be selected based on the system operating mode.

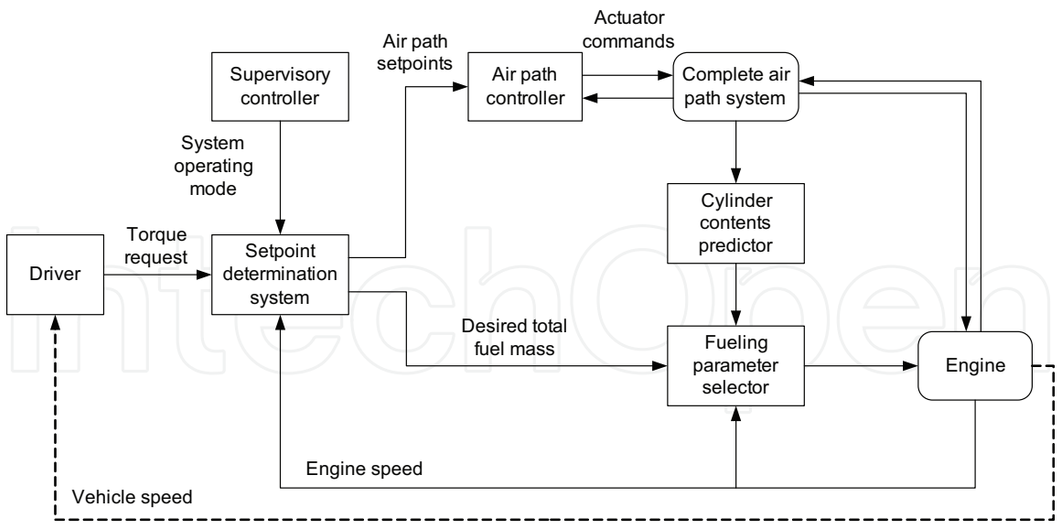

Fig. 2. Proposed air path and fueling control approach

From an engineering standpoint, the objective of a lookup table based fueling parameter selection system should be to predict the fueling parameters as accurately as possible. Although any of the numerous in-cylinder properties which affect combustion could be used as a table indexing variable, not every variable is equally viable. Logically, the factor that best predicts the variations in the optimal fueling parameters should be chosen. In this work, to identify the most appropriate variable and test the performance of the in-cylinder contents based fueling controller, a sophisticated engine model of a a six cylinder heavy-duty diesel engine was developed in the commercially available engine modeling software GT-Power.

3. GT-Power Model Description

For many in-cylinder properties such as the oxygen concentration, experimental measurements are very difficult to obtain and infeasible in a production setting. Using a high fidelity GT-Power engine model, however, the in-cylinder properties including the oxygen concentration can be predicted with reasonable confidence. A GT-Power model can accurately predict both the one-dimensional gas dynamics within an engine air path system as well as the combustion phenomena. In GT-Power, the process by which injected fuel mixes with air and combusts is based on the modeling work by Morel & Wahiduzzaman (1996). As will be shown next, a GT-Power model can predict the two most important engine performance metrics, fuel consumption and NOx emissions, quite well.

The results presented in this chapter are based on a GT-Power model of a six cylinder heavy-duty diesel engine with a variable geometry turbocharger (VGT) and an exhaust gas recirculation (EGR) system. This model was calibrated using steady-state data collected experimentally and then validated using transient data. For the steady-state calibration, each of the actuator models were tuned to ensure that the VGT and EGR actuators affect the air path in a manner consistent with the experimental data. Quantities such as the fresh air flow, EGR flow, turbine speed, exhaust pressure and intake pressure were all analyzed. Because the specific fuel consumption and NO_x production predictions are so important to the selection of the fueling parameters, particular attention was given to the predictive combustion model. The correlations between the experimental and predicted brake specific fuel consumption

(BSFC) and NO_x production are shown in Figure 3. The R^2 correlation defined by

$$R^2 = 1 - \frac{\sum_{k=1}^{n_{data}} (y_{pred} - y_{meas})^2}{\sum_{i=1}^{n_{data}} (y_{meas} - \overline{y_{meas}})^2}. \tag{1}$$

was 94.2% for the BSFC prediction and 82.9% for the NO_x prediction, both reasonably good for this type of model.

To validate the GT-Power model of the engine, the response of the model over a heavy duty FTP (Federal Test Procedure) drive cycle was compared to experimental data. In the simulation, the measured trajectories for the engine speed, the EGR valve position and the VGT position along with the command trajectories for the fueling parameters for the experimental drive cycle were imposed as inputs to the GT-Power model. For each of the relevant quantities, the predicted and experimentally measured values had very high correlations. The R^2 correlations were 91.1% for the fresh air mass flow rate, 91.3% for the EGR mass flow rate, 90.9% for the oxygen concentration of the exhaust stream and 81.1% for the NO_x production. To account for the dynamics of the NO_x sensor, the GT-Power predictions were filtered with a first order filter and then compared to the measurement data. Figure 4 depicts how well the dynamic variation in each of these four quantities is captured by the GT-Power model for the first 100 seconds of the drive cycle.

3.1 Table based fueling parameter representation comparisons

Once the GT-Power model was calibrated, a series of sensitivity studies were performed to identify the in-cylinder contents variable that has the most significant impact on the combustion process. For this study, the EGR valve position, VGT position, total fuel injection mass and engine speed were considered to be independent control variables. Approximately 20,000 different combinations of these inputs were simulated. The engine under investigation uses a pilot, a main and a post injection. Each injection is defined by two parameters, a start of injection (SOI) timing and a fuel injection quantity; however, the sum of the injection quantities must add to the desired value. At each of the 20,000 points, a total of five fueling parameters (main SOI, pilot SOI, post SOI, pilot quantity and post quantity) were optimized. This data represented steady-state operation at various altitudes as well as transient operation. It should be noted that an experimental study of this magnitude would take many months or

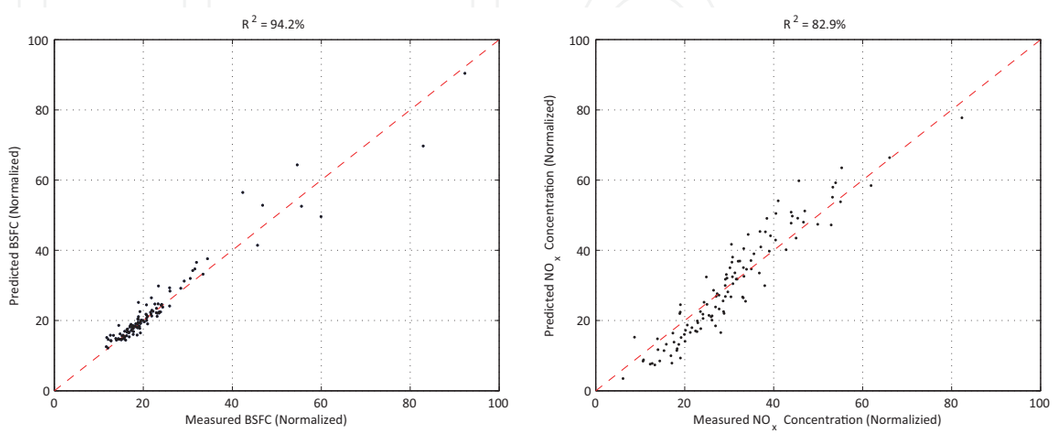

Fig. 3. Steady-state BSFC and NO_x comparisons: Experimental versus GT-Power

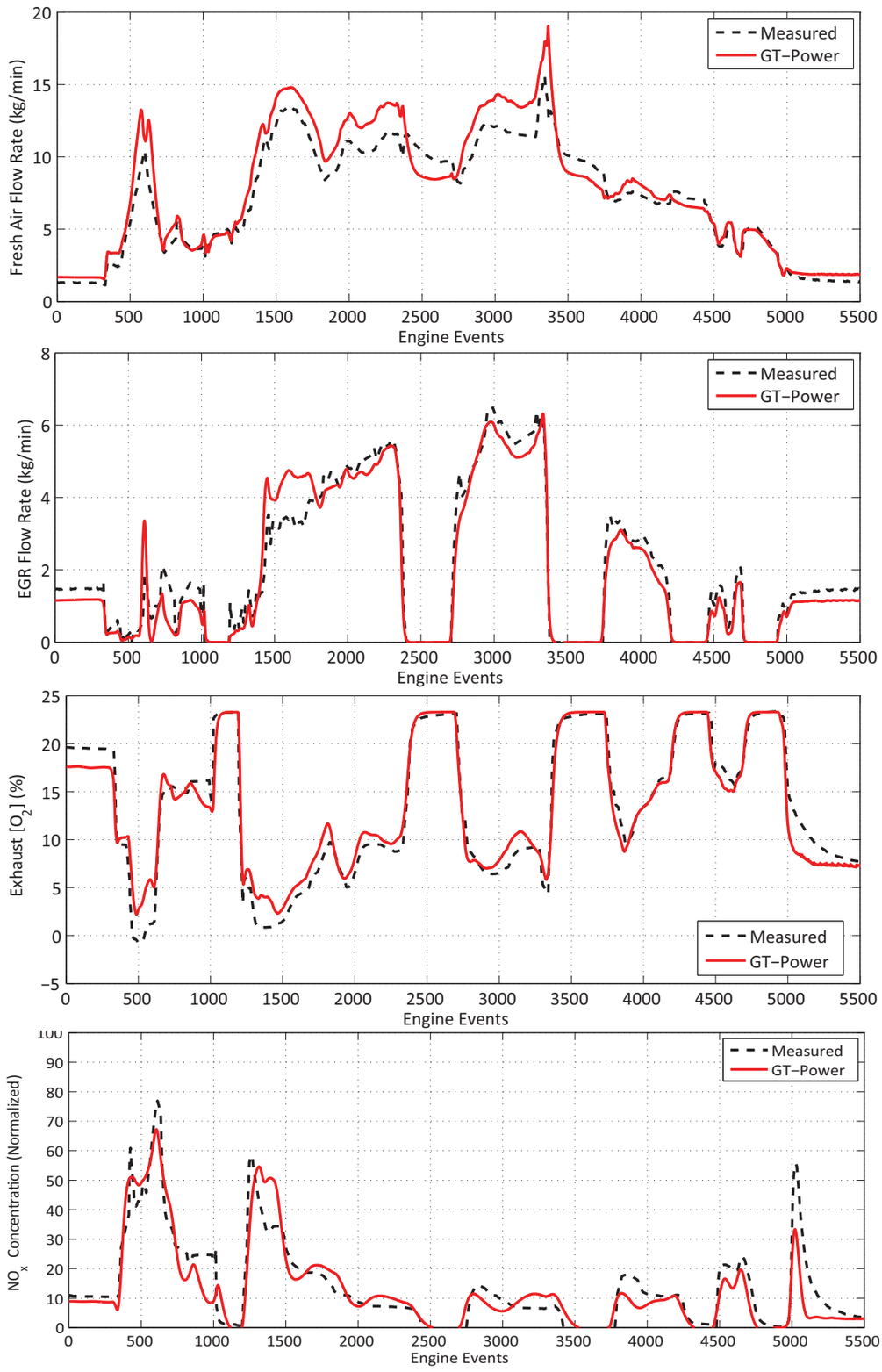

Fig. 4. Transient GT-Power model validation results

years. In a GT-Power simulation environment, however, these tests were completed in just a few weeks.

For simplicity, only two factors were considered when evaluating the engine performance, the indicated specific fuel consumption (ISFC) and the brake specific NO_x ($BSNO_x$). The calibration goal was the minimization of ISFC while limiting the $BSNO_x$ to less than 1.0 g/hp-hr. Figure 5 compares the $BSNO_x$ versus ISFC trade-off produced by the optimal set of fueling parameters to the trade-offs of alternative sets of fueling parameters for a single operating condition (1000 RPM, 65 mg fuel). Because of the proprietary nature of the data, all of the ISFC values presented in this chapter have been normalized with respect to the full range of achievable ISFC values (i.e. percentage of full scale). The 20,000 sets

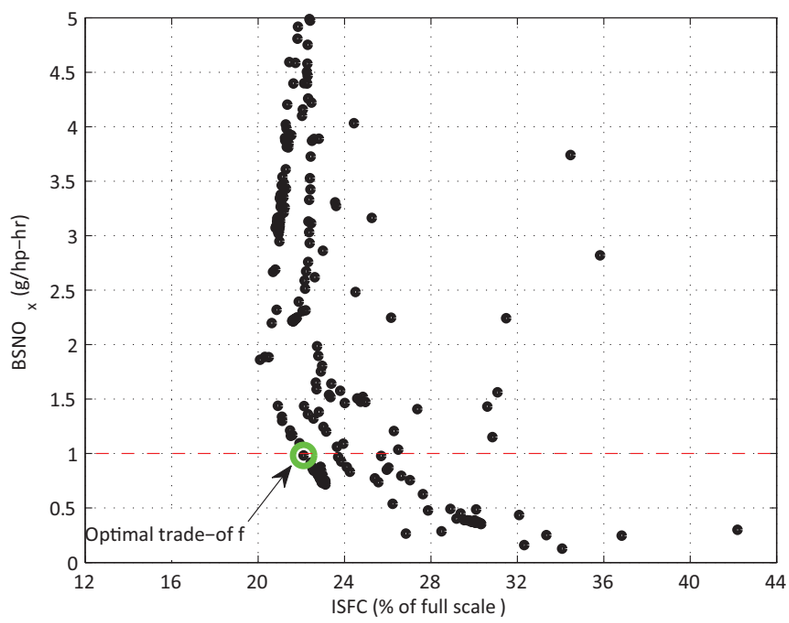

Fig. 5. Fueling parameter calibration example (1000 RPM, 65 mg fuel)

of optimal fueling parameters produced by this study were then used to calibrate sets of three-dimensional fueling parameter prediction tables, each of which used different indexing variables. Mirroring the typical approach currently in production, two of the indexing variables were select to be engine speed and fuel injection mass. For the third, the following variables were tested: total trapped charge mass, trapped oxygen mass, trapped burned gas mass, in-cylinder oxygen concentration, mass ratio of fuel to oxygen and charge density. At a minimum, three different system operating modes (steady-state, transient and altitude) are required to characterize the different modes of normal engine operation. Fundamentally, the only difference between the transient, steady-state and altitude fueling tables within a conventional controller is that they correspond to different air path setpoints. In industry, air path and fueling tables use a very fine grid spacing for the engine speed and fuel mass variables, on the order of 20 values each. Because the proposed in-cylinder contents based fueling tables cover at least three different system operating modes, the size of the three-dimensional tables was selected to be 10 x 10 x 10 to keep the total number of entries comparable to current practice.

To quantify the effectiveness of each candidate table indexing variable, the R^2 fit correlations between the table predicted fueling parameters and the optimal values of the fueling parameters were calculated. All of the correlations are presented in Table 1. The tables indexed by in-cylinder oxygen concentration (ratio of the oxygen mass to the total gas mass) best predicted the optimal fueling parameters. It is well known in the diesel engine research community that the in-cylinder oxygen concentration has a strong effect on the combustion process. As the oxygen concentration decreases due to the addition of a dilutant such as recirculated exhaust gas, the heat release rate decreases. To offset this effect, the start of combustion must be advanced by advancing the SOI timings. It is therefore not surprising that the optimal fueling parameters are strongly correlated to the in-cylinder oxygen concentration. As long as the in-cylinder oxygen concentration can be dynamically estimated, these results indicate that lookup tables indexed by engine speed, fuel mass and in-cylinder oxygen concentration can closely predict the optimal fueling parameters.

Table 1. Fueling table R^2 fit comparison (all values in %)

	Main SOI	Pilot SOI	Post SOI	Pilot Qty	Post Qty
$\frac{\text{Oxygen Mass}}{\text{Total Mass}}$	95.0	94.3	96.9	90.0	90.8
Burned Mass	94.7	93.7	94.5	84.2	85.0
Total Mass	88.4	83.5	95.9	87.9	86.4
$\frac{\text{Fuel Mass}}{\text{Oxygen Mass}}$	88.1	83.2	95.5	87.1	85.2
Oxygen mass	76.6	69.2	89.1	77.7	79.6
Charge Density	73.2	69.6	89.1	80.8	68.0

4. Delay based oxygen dynamics modeling

For an in-cylinder oxygen concentration based fueling controller to be practical, the in-cylinder oxygen concentration must be estimated reliably with a model simple enough for real time implementation in a production ECU. A wide range of real-time oxygen concentration prediction models have been studied, including models derived from the first law of thermodynamics (Ammann et al., 2003; Canova et al., 2009; van Nieuwstadt et al., 2000), linear parameter varying models (Jung & Glover, 2006; Wang, 2008; Yan & Wang, 2010), steady-state relationships (Chen & Yanakiev, 2005) and empirical models (Alberer & Del Re, 2009; Langthaler & Del Re, 2007; 2008). All of these approaches are based on zero-dimensional system descriptions and therefore do not account for the time-varying transport delays which characterize the air path system. By ignoring these delays, the predicted in-cylinder oxygen concentration tends to lead the actual oxygen concentration. Although most of these models are simple enough to be implemented in a production ECU, the oxygen concentration prediction errors can be significant, especially during rapid transients. To directly account for the time varying transport delays, a delay based oxygen dynamics model has been derived from a one-dimensional description of the air path oxygen dynamics.

Assuming a uniform radial distribution, the engine air path system can be partitioned into three one-dimensional control volumes corresponding to the exhaust, EGR and intake systems. The longitudinal oxygen dynamics within each of these systems can be described by the following one-dimensional oxygen diffusion-convention equation:

$$\frac{\partial[O_2]}{\partial t} - D\frac{\partial^2[O_2]}{\partial z^2} + v\frac{\partial[O_2]}{\partial z} + \dot{r}_{O_2} = 0, \tag{2}$$

where z is the characteristic length variable, v is the fluid velocity, $[O_2]$ is the oxygen concentration on a per mass basis, D is the diffusivity of oxygen in the gaseous mixture and $\dot{r}_{O_2}$ is the rate of oxygen is produced by chemical reactions. If all of the chemical reactions are assumed to occur inside the combustion chamber, then the oxygen production term can be eliminated. Next, the one-dimensional control volumes can be spatially discretized into many cells. Using a discretization length of Δz, this gives rise to

$$\frac{d[O_2]_i(t)}{dt} = D\frac{[O_2]_{i-1}(t) - 2[O_2]_i(t) + [O_2]_{i+1}(t)}{\Delta z^2} - v\frac{[O_2]_i(t) - [O_2]_{i-1}(t)}{\Delta z}$$

where $[O_2]_i$ is oxygen concentration of the ith control volume cell. Assuming constant cross sectional area, the oxygen dynamics equation can be rewritten in terms of the volumetric flow rate in the manner

$$\frac{d[O_2]_i(t)}{dt} = \Big(D_1 + \frac{q_{in}(t)}{V_{cell}}\Big)[O_2]_{i-1}(t) + \Big(-2D_1 - \frac{q_{in}(t)}{V_{cell}}\Big)[O_2]_i(t) + D_1[O_2]_{i+1}(t) \tag{3}$$

where

$$D_1 = \frac{D}{\Delta z^2}, \tag{4}$$

q_{in} is the volumetric flow rate entering the control volume and V_{cell} is the volume of a unit cell.

Next, this time domain oxygen concentration model can be converted into the engine event domain in which a combustion occurrence is defined as an event. In the event domain, the number of events per engine cycle is equal to the number of cylinders. One can convert between the event domain defined by variable e and the time domain defined by variable t using

$$t = \frac{120}{n_{cyl}N}e \tag{5}$$

where n_{cyl} is the number of cylinders and N is the engine speed. The derivative of this equation can be approximated as

$$dt = \frac{120}{n_{cyl}N}de, \tag{6}$$

because the rate of change of engine speed is insignificant in this setting. The volumetric flow rates can also be converted from the time domain to the event domain. Define $q^{\star}_{in}(e)$ as the volumetric flow rate entering the system on per event which satisfies

$$q^{\star}_{in}(e) = \frac{120}{n_{cyl}N}q_{in}(t). \tag{7}$$

With these relationships, the continuous time domain oxygen concentration model described by (3) can be converted to the continuous event domain model

$$\frac{n_{cyl}N}{120}\frac{d[O_2]_i(e)}{de} = \Big(D_1 + q_{in}^{\star}\frac{n_{cyl}N}{120V_{cell}}\Big)[O_2]_{i-1}(e) + \Big(-2D_1 - q_{in}^{\star}\frac{n_{cyl}N}{120V_{cell}}\Big)[O_2]_i(e) + D_1[O_2]_{i+1}(e). \tag{8}$$

By defining D_2 as

$$D_2 = \frac{120}{n_{cyl}N}D_1, \tag{9}$$

the event domain model can be reduced to

$$\frac{d[O_2]_i(e)}{de} = \Big(D_2 + \frac{q_{in}^{\star}}{V_{cell}}\Big)[O_2]_{i-1}(e) + \Big(-2D_2 - \frac{q_{in}^{\star}}{V_{cell}}\Big)[O_2]_i(e) + D_2[O_2]_{i+1}(e).$$

Applying the discrete Euler approximation with an integration step (in event space) of Δe, the changing rate of the oxygen concentration within a unit control volume can be approximated as

$$\frac{d[O_2]_i(e)}{de} \approx \frac{[O_2]_i(e+\Delta e) - [O_2]_i(e)}{\Delta e}. \tag{10}$$

With this approximation the oxygen dynamics equation becomes

$$[O_2]_i(e+\Delta e) = \Delta e\Big(D_2 + \frac{q_{in}^{\star}}{V_{cell}}\Big)[O_2]_{i-1}(e) + \Big(1 - 2\Delta e D_2 - \Delta e\frac{q_{in}^{\star}}{V_{cell}}\Big)[O_2]_i(e) + \Delta e D_2[O_2]_{i+1}(e). \tag{11}$$

When the gas velocity is sufficiently large, the diffusion effects can be ignored. Under these circumstances, the oxygen dynamics reduce to

$$[O_2]_i(e+\Delta e) = \Delta e\frac{q_{in}^{\star}}{V_{cell}}[O_2]_{i-1}(e) + \Big(1 - \Delta e\frac{q_{in}^{\star}}{V_{cell}}\Big)[O_2]_i(e). \tag{12}$$

If additionally the volumetric flow rate were constant, then the convection dynamics could be reduced to a pure transport delay by choosing a special time step Δe_1 defined as

$$\Delta e_1 = \frac{V_{cell}}{q_{in}^{\star}}. \tag{13}$$

With this choice, the oxygen concentration of the ith control volume cell can be predicted with

$$[O_2]_i(e+\Delta e_1) = [O_2]_{i-1}(e). \tag{14}$$

This result can then be extended to predict the oxygen concentration at the outlet of the subsystem $[O_2]_{outlet}$ as the following function of the oxygen concentration at the inlet of the subsystem $[O_2]_{inlet}$:

$$[O_2]_{outlet}(e+\Delta e_2) = [O_2]_{inlet}(e). \tag{15}$$

where

$$\Delta e_2 = \frac{V_{sys}}{q_{in}^{\star}}. \tag{16}$$

and V_{sys} is the total volume of the subsystem.

Using (15) and (16) to approximate the transport delays, a simple discrete time air path model can be generated. Define k as a discrete time index in engine events (i.e. $\Delta e = 1$). Nominal transport delay estimates of the exhaust system (${d_{exh}}^{\dagger}$), the EGR system (${d_{egr}}^{\dagger}$) and intake system (${d_{int}}^{\dagger}$) can be produced using

$$ {d_{exh}}^{\dagger}(k) = \frac{V_{exh} p_{exh}(k)}{\dot{m}_{exh}^{\star}(k) T_{exh}(k) R}, \tag{17}$$

$$ {d_{egr}}^{\dagger}(k) = \frac{V_{egr} p_{egr}(k)}{\dot{m}_{egr}^{\star}(k) T_{egr}(k) R}, \tag{18}$$

$$ {d_{int}}^{\dagger}(k) = \frac{V_{int} p_{int}(k)}{\left(\dot{m}_{egr}^{\star}(k) + \dot{m}_{fresh}^{\star}(k)\right) T_{int}(k) R}. \tag{19}$$

where V_{exh}, V_{egr} and V_{int} represent the volumes of the exhaust, EGR and intake systems; p_{exh}, p_{egr} and p_{int} represent the pressures within the exhaust, EGR and intake systems; T_{exh}, T_{egr} and T_{int} represent the temperatures within the exhaust, EGR and intake systems; $\dot{m}_{egr}^{\star}$ represents the EGR mass flow rate on a per event basis and $\dot{m}_{fresh}^{\star}$ represents the mass flow rate of fresh air on a per event basis. Although these estimates assume the gas velocities within each system are constant (which may not always be the case), this method of estimating the transport delays is much more accurate than current methods which ignore the delays altogether. Through the use of memory buffers, these nominal delays can be used to predict the oxygen concentrations leaving the exhaust, EGR and intake systems based on the oxygen concentrations entering these systems. Before these delay estimates can be used, they must be converted to integers and bounded to account for the fixed allocation of memory. With the following three equations, the nominal exhaust, EGR and intake delays can be converted into integer delays:

$$ d_{exh}(k) = \begin{cases} \lfloor {d_{exh}}^{\dagger}(k) \rfloor & \text{if } {d_{exh}}^{\dagger}(k) < d_{exh,max} \\ d_{exh,max} & \text{otherwise} \end{cases}, \tag{20}$$

$$ d_{egr}(k) = \begin{cases} \lfloor {d_{egr}}^{\dagger}(k) \rfloor & \text{if } {d_{egr}}^{\dagger}(k) < d_{egr,max} \\ d_{egr,max} & \text{otherwise} \end{cases} \tag{21}$$

and

$$ d_{int}(k) = \begin{cases} \lfloor {d_{int}}^{\dagger}(k) \rfloor & \text{if } {d_{int}}^{\dagger}(k) < d_{int,max} \\ d_{int,max} & \text{otherwise} \end{cases} \tag{22}$$

where $d_{exh,max}$ is the largest allowable exhaust system transport delay, $d_{egr,max}$ is the largest allowable EGR system transport delay and $d_{int,max}$ is the largest allowable intake system transport delay.

During each event new exhaust gas enters the EGR system. The oxygen concentration of the gases leaving the EGR system depends on the oxygen concentration of the gases currently in the EGR system and the oxygen concentration of the exhaust gases that enter the EGR system. Because of transport delay, the oxygen concentration of the gases entering the system depends on the oxygen concentration of the exhaust gas that was expelled several events

prior. Accordingly, the nominal oxygen concentration at the confluence function where the EGR system meets the intake system ${[O_2]_{egr}}^{\dagger}$ can be approximated with

$$
\begin{aligned}
{[O_2]_{egr}}^{\dagger}(k) = {[O_2]_{exh}}^{\dagger}\big(k - d_{exh}(k) - d_{egr}(k)\big)\frac{\dot{m}^{\star}_{egr}(k)}{\epsilon\,\dot{m}^{\star}_{egr,max}} \\
+{[O_2]_{egr}}^{\dagger}(k-1)\frac{\epsilon\,\dot{m}^{\star}_{egr,max} - \dot{m}^{\star}_{egr}(k)}{\epsilon\,\dot{m}^{\star}_{egr,max}}
\end{aligned}
\tag{23}
$$

where ${[O_2]_{exh}}^{\dagger}$ is the nominal oxygen concentration at the exhaust ports, $\dot{m}^{\star}_{egr,max}$ is the maximum possible mass flow rate of EGR and $\epsilon > 1$ captures the diffusion phenomena. In the same manner, the oxygen concentration at the intake ports depends on the oxygen concentrations of the ambient air and the gases leaving the EGR system, time-shifted to account for the transport delay of the intake system. Using their respective mass flow rates as weighting factors, the nominal oxygen concentration at the intake ports, ${[O_2]_{int}}^{\dagger}$, can be modeled according to

$$
{[O_2]_{int}}^{\dagger}(k) = \frac{{[O_2]_{egr}}^{\dagger}\big(k - d_{int}(k)\big)\dot{m}^{\star}_{egr}\big(k - d_{int}(k)\big) + [O_2]_{amb}\dot{m}^{\star}_{fresh}\big(k - d_{int}(k)\big)}{\dot{m}^{\star}_{egr}\big(k - d_{int}(k)\big) + \dot{m}^{\star}_{fresh}\big(k - d_{int}(k)\big)}
\tag{24}
$$

where $[O_2]_{amb}$ is the oxygen concentration of the ambient air.

The nominal in-cylinder oxygen concentration depends on the oxygen concentration of the air charge entering the cylinders and the residual gas left in the cylinders. Define the trapped residual fraction γ_{res} as the ratio of the trapped residual mass $\dot{m}^{\star}_{res}$ to the total trapped mass $\dot{m}^{\star}_{trapped}$ as in

$$
\gamma_{res}(k) = \frac{\dot{m}^{\star}_{res}(k)}{\dot{m}^{\star}_{trapped}(k)}.
\tag{25}
$$

Using this definition, the total trapped mass $\dot{m}^{\star}_{trapped}$ can be related to the mass flow rate into the engine with

$$
m^{\star}_{trapped}(k) = \frac{\dot{m}^{\star}_{egr}\big(k - d_{int}(k)\big) + \dot{m}^{\star}_{fresh}\big(k - d_{int}(k)\big)}{1 - \gamma_{res}(k)}.
\tag{26}
$$

By assuming the trapped residual gases are equivalent to the gases that were just exhausted, the nominal in-cylinder oxygen concentration, ${[O_2]_{cyl}}^{\dagger}$, can be approximated by

$$
{[O_2]_{cyl}}^{\dagger}(k) = \big(1 - \gamma_{res}(k)\big){[O_2]_{int}}^{\dagger}(k) + {[O_2]_{exh}}^{\dagger}(k)\gamma_{res}(k).
\tag{27}
$$

Define $d_{int,exh}$ as the fixed delay between the induction and exhaust strokes. After $d_{int,exh}$ events, the inducted cylinder contents are burned and expelled into the exhaust system; therefore, the oxygen concentration at the exhaust ports can be predicted with

$$
{[O_2]_{exh}}^{\dagger}(k + d_{int,exh}) = \frac{[O_2]^{\dagger}_{cyl}(k)m^{\star}_{trapped}(k) - OFR_s m^{\star}_{fuel}(k)}{m^{\star}_{trapped}(k) + m^{\star}_{fuel}(k)}
\tag{28}
$$

where OFR_s is the stoichiometric mass ratio of oxygen to fuel. When estimating the transport delays, the nominal values are always rounded down. As a result, the in-cylinder oxygen concentration predicted in (27) tends to underestimate the total transport delay of the exhaust gas recirculation loop. To compensate for this effect and to remove any artificial jaggedness, a final in-cylinder oxygen concentration estimate $[O_2]_{cyl}$ can be predicted by filtering the nominal in-cylinder oxygen concentration according to

$$[O_2]_{cyl}(k) = \beta[O_2]_{cyl}{}^{\dagger}(k) + (1-\beta)[O_2]_{cyl}(k-1) \tag{29}$$

where β is the filter constant. To test the performance of this methodology, a delay based oxygen dynamics model was implemented into the GT-Power model of the six cylinder diesel engine. The oxygen dynamics model was then used to predict the in-cylinder oxygen concentration and the exhaust oxygen concentration over the first 100 seconds of a heavy duty FTP drive cycle. The delay based oxygen dynamics model produces excellent performance as shown in Figure 6. The top plot in Figure 6 compares the in-cylinder oxygen concentration predicted by GT-Power to the in-cylinder oxygen concentration predicted by the delay based oxygen dynamics model, whereas the bottom plot compares the predicted oxygen concentration at the exhaust ports. By directly predicting the transport delay, the oxygen concentrations predicted by a delay based oxygen dynamics model are always in phase with the actual oxygen concentrations. The root mean squared (RMS) errors in predicting the oxygen concentrations inside the cylinders and at the exhaust ports were 0.112% and 0.424% respectively. A delay based oxygen dynamics model achieves remarkable accuracy but is simple enough to be implemented in a production ECU.

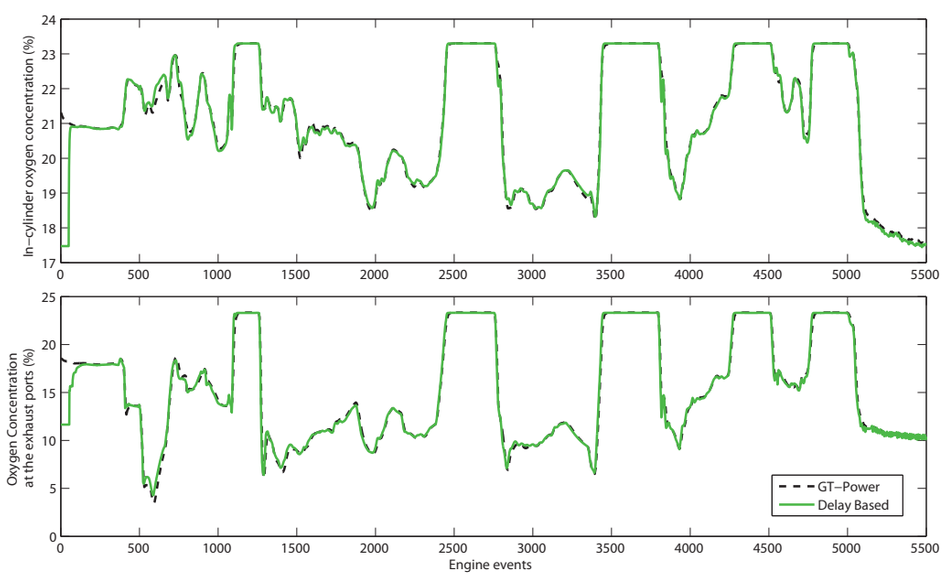

Fig. 6. Oxygen concentration prediction comparison: GT-Power versus delay based oxygen dynamics model

5. Transient performance comparison

Following the control structure shown in Figure 2, an in-cylinder oxygen concentration based fueling controller was implemented in GT-Power. Within this controller, the five fueling parameters (main SOI, pilot SOI, post SOI, pilot quantity and post quantity) are predicted with five sets of 10 x 10 x 10 tables indexed by the engine speed, the total fueling mass and the in-cylinder oxygen concentration. The in-cylinder oxygen concentration is dynamically predicted using a delay based oxygen dynamics model, whereas the exact values for the total fueling and engine speed are used directly. To provide a benchmark, a conventional fueling controller based on five sets of 20 x 20 tables indexed by the total fueling mass and the engine speed was also implemented into a separate GT-Power model.

Ideally, an air path controller would perfectly regulate the air path variables to their desired setpoints. To represent this scenario, the optimal air path actuator trajectories were directly specified and both fueling controllers were simulated in GT-Power for the first 100 seconds of a heavy duty FTP drive cycle. Under these conditions, both of the fueling control structures produced similar results. Figure 7 compares the instantaneous ISFC produced by the optimal fueling parameters to the instantaneous ISFC produced by the fueling parameters selected by the oxygen concentration based fueling controller and the conventional fueling controller. Similarly, Figure 8 compares the instantaneous $BSNO_x$ performance. It should be noted that for some sections of this drive cycle it was not possible to simultaneously meet the driver's torque request and produce a $BSNO_x$ level below 1.0 g/hp-hr. In these situations, the $BSNO_x$ level was minimized as much as possible while still achieving the desired torque. The spans of events without data correspond to decelerations where no fuel was injected. Neither controller was able to perfectly predict the optimal fueling parameters, thus resulting in small differences in the instantaneous values of ISFC and $BSNO_x$. However, these differences do not significantly affect the overall drive cycle performance.

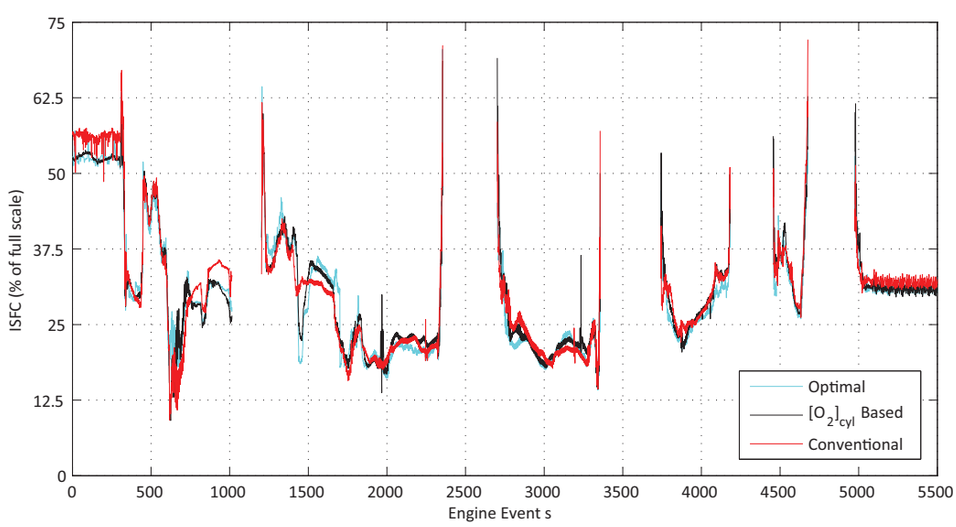

Fig. 7. ISFC Comparison: Ideal air path response

The drive cycle averaged ISFC and $BSNO_x$ results are reported in Table 2. With respect to the benchmark set by the optimal fueling parameters, the average ISFC in percentage of full scale produced by the oxygen concentration based fueling controller was 0.44% larger and the

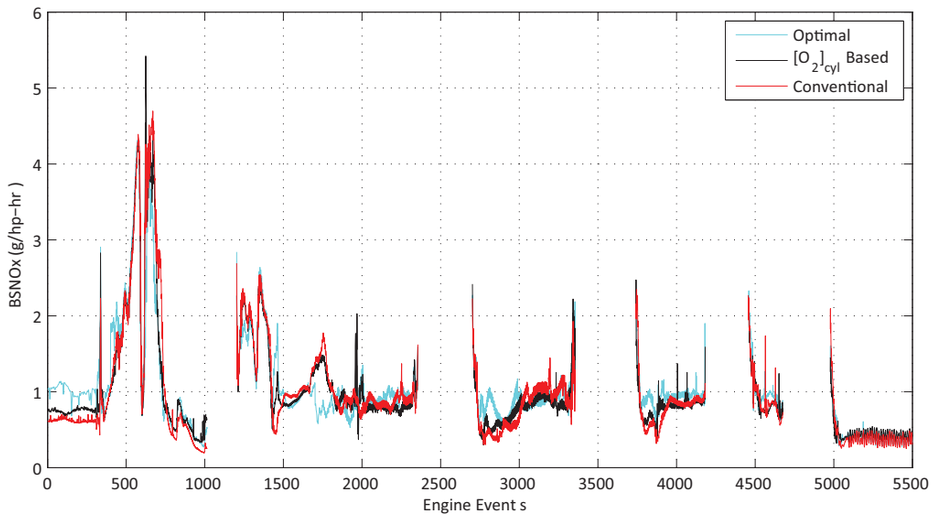

Fig. 8. BSNOx Comparison: Ideal air path response

average ISFC produced by the conventional fueling controller was 0.69% larger. Because of the inverse relationship between ISFC and $BSNO_x$, both the oxygen concentration based fueling controller and the conventional fueling controller produced on average less NO_x than the optimal fueling parameters. Recall that the optimization objective of the fueling parameter calibration was to minimize the ISFC under the constraint that the $BSNO_x$ is less than 1.0 g/hp-hr. Even though the two fueling controllers produced less NO_x on average, the optimal fueling parameters met the $BSNO_x$ target more consistently. For the oxygen concentration based fueling controller, 1.07% fewer combustion events achieved a $BSNO_x$ value less than 1.2 g/hp-hr, as compared to the optimal fueling parameters. For the conventional controller, 1.59% fewer combustion events met this criteria.

	ISFC (% of full scale)	BSNOx (g/hp-hr)	% of data with BSNOx < 1.2 g/hp-hr
Optimal	29.75	0.970	83.6%
$[O_2]_{cyl}$ Based	30.19	0.942	82.5%
Conventional	30.44	0.939	82.0%

Table 2. Drive cycle averaged combustion performance results: Ideal air path response

Although both the oxygen concentration based fueling controller and the conventional fueling controller produced on average higher values of ISFC and exceeded a $BSNO_x$ value of 1.2 g/hp-hr more frequently, the magnitude of these differences was very small for both controllers. For the in-cylinder oxygen concentration based fueling controller, these results demonstrate that the sets of three-dimensional tables indexed by engine speed, total fuel mass and in-cylinder oxygen concentration effectively predict the optimal fueling parameters and that the in-cylinder oxygen concentration prediction errors are practically negligible. In these types of ideal conditions where the trajectories of the air path setpoint variables are perfectly achieved, a conventional fueling controller with two-dimensional tables also effectively predicts the fueling parameters.

In practice, the instantaneous values of the air path setpoint variables will often differ from their desired values. Although a closed loop air path controller is designed to minimize this difference, many factors can limit the convergence rate or altogether prevent a desired value from being achieved. These factors include component failure, turbocharger surge/choke behavior, imposed air to fuel ratio limits and, most importantly, the dynamics of the air path system. To compare the robustness of an in-cylinder oxygen concentration based fueling controller to a conventional fueling controller with respect to these types of errors, the same drive cycle was simulated but with slightly different air path responses. Uniform bias shifts

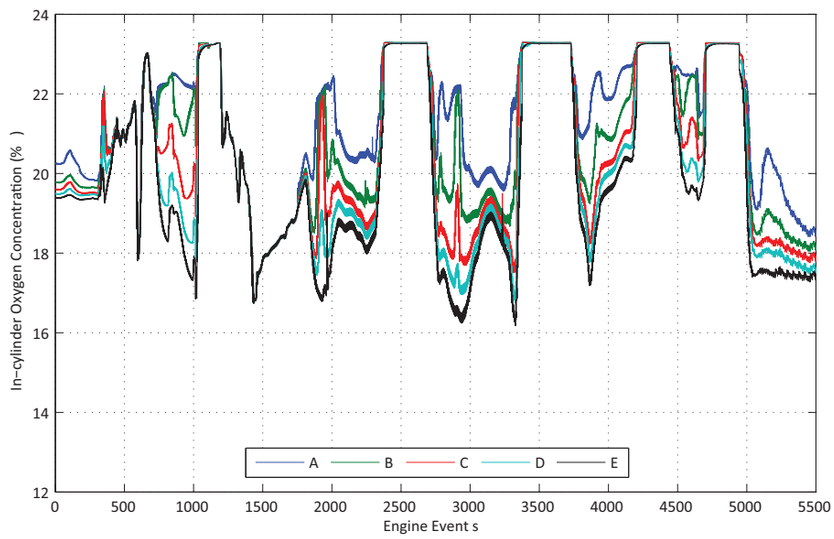

Fig. 9. In-cylinder oxygen concentration variations: Cases A - E

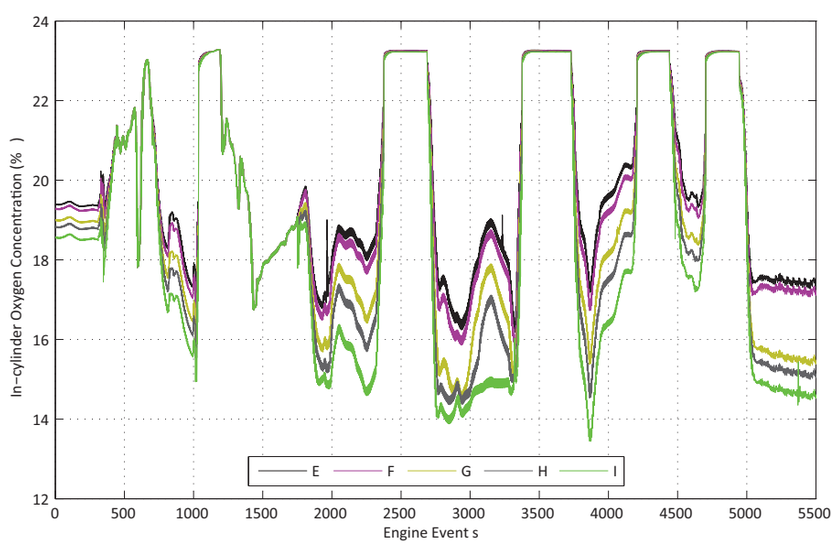

Fig. 10. In-cylinder oxygen concentration variations: Cases E - I

		$[O_2]_{cyl}$ Based		Conventional	
Case	$[O_2]_{cyl}$ (%)	ISFC (% of full scale)	$BSNO_x$ (g/hp-hr)	ISFC (% of full scale)	$BSNO_x$ (g/hp-hr)
A	20.57	41.38	1.758	32.31	2.788
B	19.95	36.06	1.367	31.00	1.907
C	19.43	32.56	1.138	30.44	1.369
D	19.07	31.06	1.020	30.31	1.102
E	18.74	30.19	0.942	30.44	0.939
F	18.53	30.32	0.875	31.13	0.839
G	17.72	30.94	0.826	33.75	0.631
H	17.36	32.06	0.778	36.06	0.562
I	16.82	34.75	0.711	41.06	0.493

Table 3. Drive cycle averaged combustion performance results: Shifted air path actuator commands

were applied to the actuator position trajectories to produces these differences. A total of eight additional drive cycles were simulated for each controller.

The actuator shifts applied to the first four drive cycles labeled “A", “B", “C" and “D" decreased the EGR flow rate and increased the fresh air flow rate. The resulting effects on the in-cylinder oxygen concentration are shown in Figure 9. The ideal case tested previously is labeled as case “E". For the remaining four tests labeled “F", “G", “H" and “I," the shifts applied to the actuator commands caused a relative increase in the EGR flow rate. Figure 10 depicts the in-cylinder oxygen concentrations resulting from these shifts. The types of uniform bias errors simulated in these tests are not meant to represent typical air path errors; rather, they were selected to help identify the robustness of each controller.

All of the drive cycle averaged results are compiled in Table 3. This same data is also visually depicted in Figure 11. These results clearly show that the two fueling controllers respond to actuator bias errors differently. Because a conventional fueling controller does not consider the state of the air path system, the conventional fueling controller responded exactly the same for each drive cycle. Although this response produced excellent performance when the air path setpoint trajectories were perfectly tracked, this same response produced poor performance when the air path setpoints were not achieved.

In general, as the in-cylinder oxygen concentration decreases (i.e. dilutent concentration increases), the heat release rate decreases. To offset this effect, the fuel injection timing should be advanced. Conversely, as the oxygen concentration increases (i.e. diluent concentration decreases), the combustion temperature tends to increase, thus increasing the NO_x production rate. To prevent this increase, the fuel injection timings should be retarded. These types of corrective actions are not applied by a conventional fueling controller. For drive cycles (A, B, C, D) with actuator biases which cause an increase in the in-cylinder oxygen concentration, the conventional fueling controller consistently injected fuel sooner than it should, resulting in drastically higher $BSNO_x$ values. On the other hand, for drive cycles (F, G, H, I) with actuator biases which cause a decrease in the in-cylinder oxygen concentration, the conventional fueling controller consistently injected fuel later than it should, resulting in larger ISFC values.

With an in-cylinder oxygen concentration based fueling controller, the changes to the oxygen concentration caused by the air path actuator biases are correctly compensated. Based on the

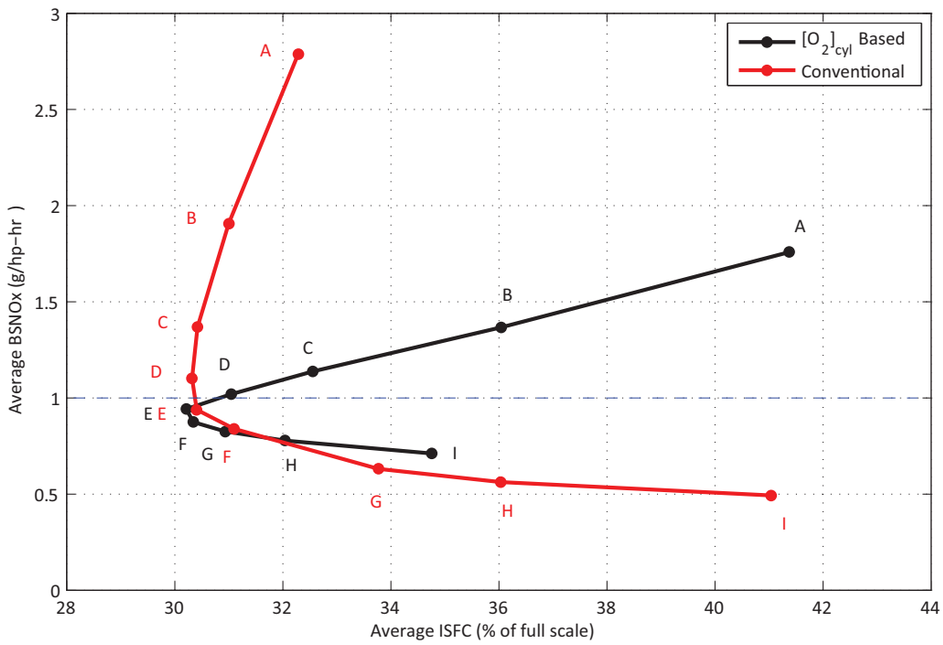

Fig. 11. Trade-off between cycle averaged $BSNO_x$ and cycle average ISFC

objective function used to calibrate the controller, the in-cylinder oxygen concentration based fueling controller produces a nearly constant NO_x production rate of about 1 g/hp-hr. Under certain conditions, however, this target NO_x production rate cannot be achieved through fuel injection adjustments alone. In these cases, the oxygen concentration based fueling controller selects the fueling parameters that minimize the $BSNO_x$ while meeting the torque request. For the drive cycles in which the EGR flow rate was decreased (A, B, C, D), these types of conditions were encountered more frequently.

To further illustrate these effects, the ISFC and $BSNO_x$ values produced by the two controllers have been directly compared on an event-by-event basis to generate families of probability density functions. The magnitude of the difference in the ISFC values achieved by the two fueling controllers depends on the magnitude of the air path setpoint errors. This is also true for the $BSNO_x$ difference. Figure 12 depicts how the distribution of the ISFC difference between the conventional fueling controller and the oxygen concentration based fueling controller varied as a function of the in-cylinder oxygen concentration difference (achieved value minus the value corresponding to the optimal air path setpoints). The median ISFC difference is also included in this figure on the bottom plane (i.e. 0% probability). Each of the probability density functions corresponds to a particular oxygen concentration difference. The random variable responsible for these variations corresponds to the combined effects of engine speed, the fuel injection mass and the cylinder conditions.

When the oxygen concentration difference for a given combustion event was approximately -2%, for example, the ISFC produced by the conventional controller was between 0% and 15% larger than the ISFC produced by the oxygen concentration based fueling controller for 91.9% of the occurrences. This same information can be extracted from Figure 12 by integrating the

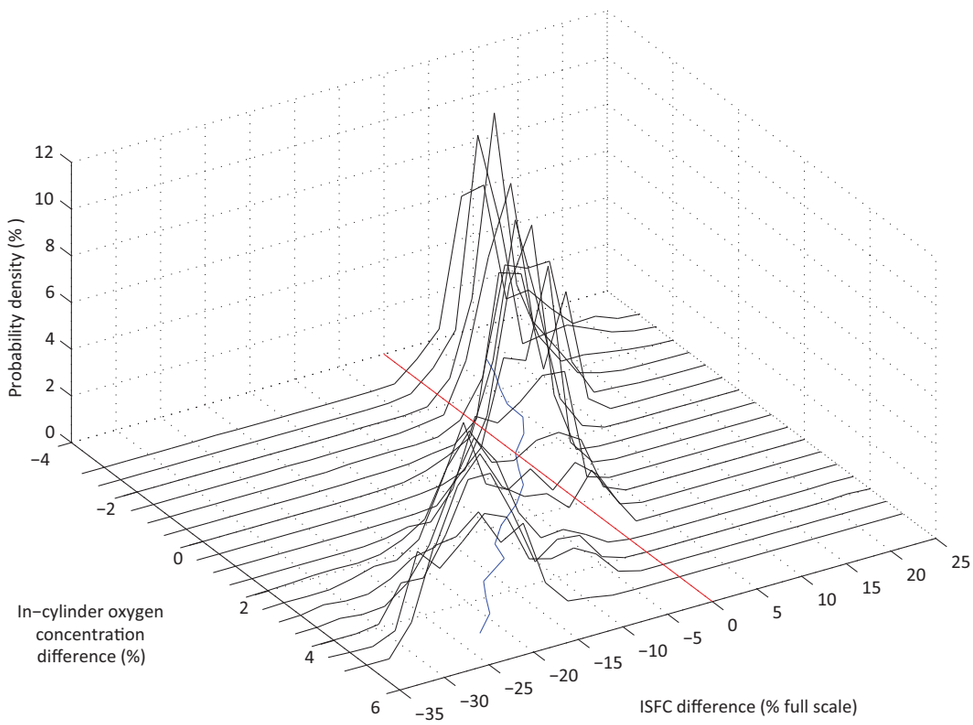

Fig. 12. Instantaneous ISFC difference (Conventional - $[O_2]_{cyl}$ based) probability density functions

probability density function curve corresponding to an oxygen concentration difference of -2% from 0% to 15%. Each of the distributions has approximately the same degree of narrowness indicating that the compensatory adjustments made by an in-cylinder oxygen concentration based fueling controller influence the combustion performance in a consistent manner.

A similar set of probability density functions shown in Figure 13 were created to illustrate how the $BSNO_x$ difference between the conventional fueling controller and the oxygen concentration based fueling controller varies as a function of the in-cylinder oxygen concentration difference. These probability density functions are also characterized by very narrow distributions. For negative oxygen concentration differences, the two controllers tended to produce approximately the same $BSNO_x$. When the oxygen concentration difference is positive, an in-cylinder oxygen concentration based fueling control produced significantly less NO_x. In fact, the magnitude of these changes was frequently larger than 1.0 g/hp-hr. These conditions correspond to combustion events where the oxygen concentration based fueling controller remained near the $BSNO_x$ target of 1.0 g/hp-hr while the conventional fueling controller produced more than double that same target.

The occurrence frequency of each (ISFC, $BSNO_x$) pair encountered across all of the drive cycle simulations has also been analyzed for each control structure. Figures 14 and 15 depicts the result on a logarithmic scale. To put this data in perspective, the drive cycle averaged (ISFC, $BSNO_x$) pairs originally presented in Figure 5 have also been superimposed

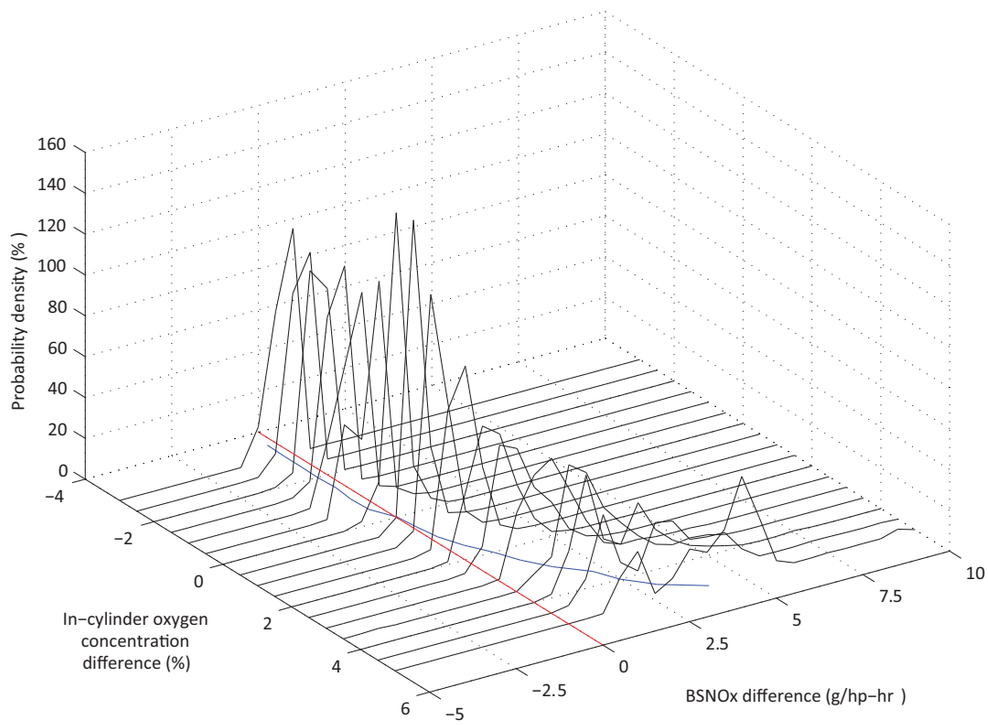

Fig. 13. Instantaneous $BSNO_x$ difference (Conventional - $[O_2]_{cyl}$ based) probability density functions

into these distribution charts as white curves. The combustion produced by the in-cylinder oxygen concentration based controller most frequently resulted in (ISFC, $BSNO_x$) pairs within the range [18, 35] % × [0.4, 1.4] g/hp-hr. Conversely, the combustion produced by the conventional controller most frequently resulted in a wider range of (ISFC, $BSNO_x$) pairs contained within the box outlined by [18, 40] % × [0.1, 1.7] g/hp-hr. Moreover, the $BSNO_x$ produced by the oxygen concentration based fueling controller for almost all of the combustion events was below 4.5 g/hp-hr, whereas this $BSNO_x$ exceeded 4.5 g/hp-hr on numerous occasions with the conventional fueling controller.

		$[O_2]_{cyl}$ Based		Conventional	
Case	$[O_2]_{cyl}$ (%)	ISFC (% of full scale)	$BSNO_x$ (g/hp-hr)	ISFC (% of full scale)	$BSNO_x$ (g/hp-hr)
J	18.55	32.75	0.925	33.38	1.007
K	18.67	33.44	0.972	33.50	1.115
L	18.12	34.38	0.982	36.88	1.040
M	18.70	35.69	1.133	36.06	1.745

Table 4. Drive cycle averaged combustion performance results: Dynamic air path actuator errors

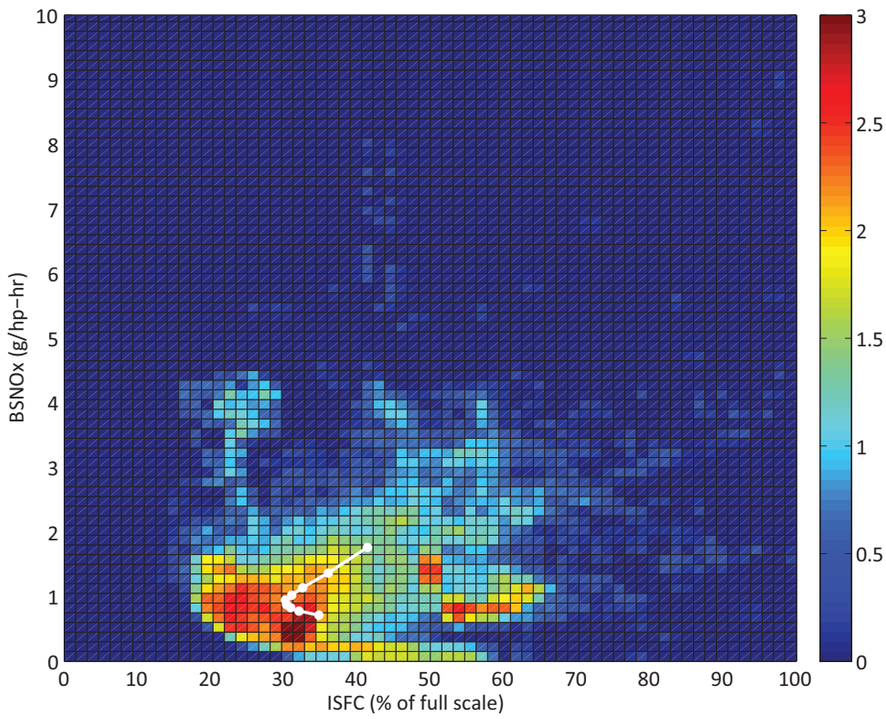

Fig. 14. Distribution of (ISFC, $BSNO_x$) pairs for the oxygen concentration based fueling controller

In contrast to the constant bias errors tested thus far, most air path errors are transient in nature. The relative performance of the two fueling controllers depends on the air path trajectory, so an infinite number of air path error trajectories are possible. To demonstrate some of the possible outcomes, a few hypothetical dynamic air path error trajectories have been simulated. The first two cases labeled "J" and "K" had dynamic errors which are approximately of the same order as those seen experimentally. The second two cases labeled "L" and "M" contained larger dynamic errors (both in amplitude and duration). The drive cycle averaged performance results for these drive cycles are assembled in Table 4. The cycle averaged (ISFC, $BSNO_x$) pairs are also plotted in Figure 16. Included for reference are the cycle averaged data pairs for drive cycles A through I.

For each of the four drive cycles, the in-cylinder oxygen concentration based fueling controller produced more desirable combustion performance than the conventional fueling controller in terms of both fuel consumption and NO_x production. Between the two cases which simulated moderate dynamic air path errors, the cycle averaged ISFC achieved by the oxygen concentration fueling controller in percentage of full scale was as much as 0.63% lower than the conventional fueling controller. The oxygen concentration based fueling controller also reduced the cycle averaged $BSNO_x$ by as much as 0.143 g/hp-hr. The larger dynamic errors simulated in cases L and M produced even larger relative changes. Under these conditions, the cycle averaged ISFC produced by the oxygen concentration based fueling controller in percentage of full scale was as much as 2.50% lower than the conventional fueling controller and the cycle averaged $BSNO_x$ was decreased by much as 0.612 g/hp-hr.

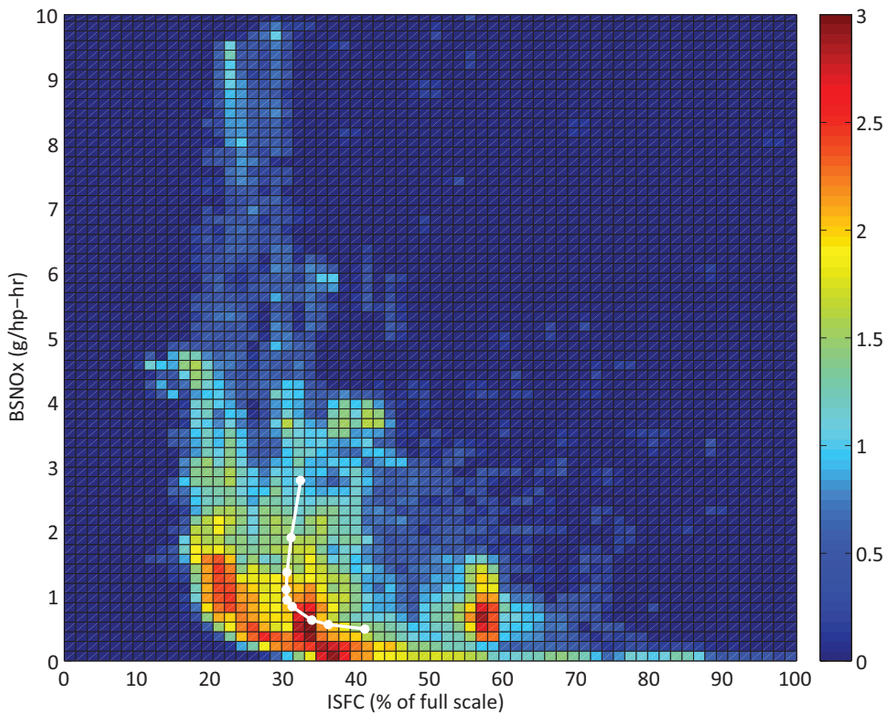

Fig. 15. Distribution of (ISFC, $BSNO_x$) pairs for the conventional fueling controller

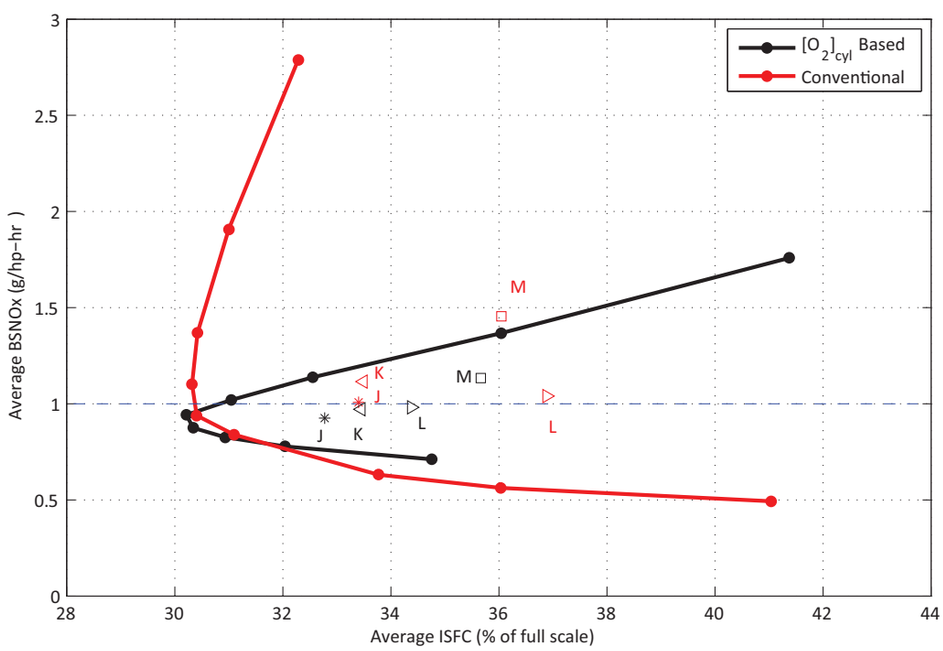

Fig. 16. Trade-off between cycle averaged $BSNO_x$ and cycle averaged ISFC: Dynamic air path errors

6. Conclusions

Modern diesel engines have sophisticated fuel injection systems that allow for multiple fuel injection pulses, thus providing flexibility in shaping the combustion process. The timing of each of these injections and fraction of the total fuel delivered by each injection can be modified to ensure that the combustion produces a desired trade-off between performance metrics. A typical diesel engine controller determines both the desired air path setpoints and the fueling parameters based on a feed-forward mapping of the engine speed, the fuel injection mass and the system operating mode. The main difference between different system operating modes such as transient, steady-state and altitude is that they require different air path setpoints to achieve the desired level of performance. The combustion process depends on quantities within the cylinder after the intake valve closes, and not on how those quantities got there. Provided they can be estimated, scheduling the fuel injection parameters on the in-cylinder conditions rather than the system operating mode is a more robust and effective solution.

The air path of a diesel engine, including the intake manifold, exhaust manifold and the exhaust gas recirculation loop is characterized by mass accumulation and mass transport dynamics. Without a thorough understanding of these dynamics, the in-cylinder content cannot be estimated accurately. Beginning from the one-dimensional oxygen diffusion-convention equation, a delay based oxygen dynamics model capable of dynamically predicting the in-cylinder oxygen concentration was designed and demonstrated in this chapter. This model is quite simple and could be run in real time in a production ECU. Enabled by the delay based oxygen dynamics model, an in-cylinder oxygen concentration based fueling controller was also developed. The resulting in-cylinder oxygen concentration based fueling controller demonstrated in simulation the ability to consistently limit the $BSNO_x$ to below a desired level while minimizing the ISFC and smoothly meeting the torque request. In steady-state, the performance of an oxygen concentration based fueling controller is equivalent to a conventional controller. During a transient, however, the robustness provided by scheduling the fueling parameters based on the in-cylinder oxygen concentration allows the fueling controller to maintain any desired set of performance trade-offs. Even when a component within the air path system fails or when exceptional control action is taken to prevent the turbocharger system from reaching its surge or choke limits, an oxygen concentration based fueling controller achieves very good performance.

7. References

Alberer, D. & Del Re, L. (2009). Fast oxygen based transient diesel engine operation, *SAE International Journal of Engines* 2(1): 405–413. No. 2009-01-0622.

Ammann, M., Fekete, N. P., Guzzella, L. & Glattfelder, A. H. (2003). Model-based control of the VGT and EGR in a turbocharged common-rail diesel engine: Theory and passenger car implementation, *SAE*. No. 2003-01-0357.

Benajes, J., Molina, S. & Garcia, J. (2001). Influence of pre- and post-injection on the performance and pollutant emissions in a HD diesel engine, *SAE*. No. 2001-01-0526.

Canova, M., Midlam-Mohler, S., Guezennec, Y. & Rizzoni, G. (2009). Mean value modeling and analysis of HCCI diesel engines with external mixture formation, *Journal of Dynamic Systems, Measurements, and Control* 131: 011002–1 – 011002–14.

Chen, S. K. & Yanakiev, O. (2005). Transient NOx emissions reduction using exhaust oxygen concentration based control for a diesel engine, *SAE*. No. 2005-01-0372.

Guzzella, L. & Amstutz, A. (1998). Control of diesel engines, *IEEE Control Systems Magazine* pp. 53–71.

Jung, M. & Glover, K. (2006). Calibratable linear parameter-varying control of a turbocharged diesel engine, *IEEE Transactions on Control Systems Technology* 14(1): 45–62.

Langthaler, P. & Del Re, L. (2007). Fast predictive oxygen charge control of a diesel engine, *Proceedings of the 2007 American Control Conference*.

Langthaler, P. & Del Re, L. (2008). Robust model predictive control of a diesel airpath, *Proceedings of the 2008 International Federation of Automatic Control*.

MacMillan, D., La Rocca, A., Shayler, P. J., Morris, T., Murphy, M. & Pegg, I. (2009). Investigating the effects of multiple injections on stability at cold idle for DI diesel engines, *SAE*. No. 2009-01-0612.

Morel, T. & Wahiduzzaman, S. (1996). Modeling of diesel combustion and emissions, *XXVI FISITA Congress*.

Osuka, I., Nishimura, M. & Tanaka, Y. (1994). Benefits of new fuel injection system technology on cold startability of diesel enginess, *SAE*. No. 940586.

van Nieuwstadt, M. J., Kolmanovsky, I. V. & Moraal, P. E. (2000). Coordinated EGR-VGT control for diesel engines: an experimental comparison, *SAE*. No. 2000-01-0266.

Wang, J. (2008). Air fraction estimation for multiple combustion mode diesel engines with dual-loop EGR systems, *Control Engineering Practice* 16: 1479–1486.

Yan, F. & Wang, J. (2010). In-cylinder oxygen mass fraction cycle-by-cycle estimation via a Lyapunov-based observer design, *Proceedings of the 2010 American Control Conference*.

IntechOpen

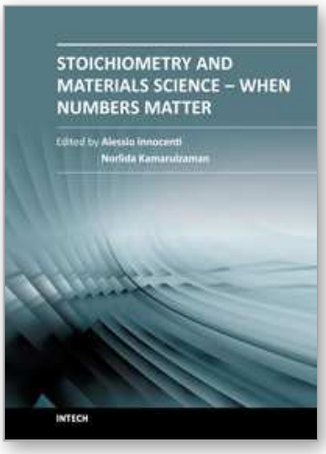

Stoichiometry and Materials Science - When Numbers Matter

Edited by Dr. Alessio Innocenti

ISBN 978-953-51-0512-1

Hard cover, 436 pages

Publisher InTech

Published online 11, April, 2012

Published in print edition April, 2012

The aim of this book is to provide an overview on the importance of stoichiometry in the materials science field. It presents a collection of selected research articles and reviews providing up-to-date information related to stoichiometry at various levels. Being materials science an interdisciplinary area, the book has been divided in multiple sections, each for a specific field of applications. The first two sections introduce the role of stoichiometry in nanotechnology and defect chemistry, providing examples of state-of-the-art technologies. Section three and four are focused on intermetallic compounds and metal oxides. Section five describes the importance of stoichiometry in electrochemical applications. In section six new strategies for solid phase synthesis are reported, while a cross sectional approach to the influence of stoichiometry in energy production is the topic of the last section. Though specifically addressed to readers with a background in physical science, I believe this book will be of interest to researchers working in materials science, engineering and technology.

How to reference

In order to correctly reference this scholarly work, feel free to copy and paste the following:

Jason Meyer and Stephen Yurkovich (2012). Improved Combustion Control in Diesel Engines Through Active Oxygen Concentration Compensation, Stoichiometry and Materials Science - When Numbers Matter, Dr. Alessio Innocenti (Ed.), ISBN: 978-953-51-0512-1, InTech, Available from: http://www.intechopen.com/books/stoichiometry-and-materials-science-when-numbers-matter/improved-combustion-control-in-diesel-engines-through-active-oxygen-concentration-compensation

INTECH
open science | open minds

InTech Europe
University Campus STeP Ri
Slavka Krautzeka 83/A
51000 Rijeka, Croatia
Phone: +385 (51) 770 447
Fax: +385 (51) 686 166
www.intechopen.com

InTech China
Unit 405, Office Block, Hotel Equatorial Shanghai
No.65, Yan An Road (West), Shanghai, 200040, China
中国上海市延安西路65号上海国际贵都大饭店办公楼405单元
Phone: +86-21-62489820
Fax: +86-21-62489821

© 2012 The Author(s). Licensee IntechOpen. This is an open access article distributed under the terms of the Creative Commons Attribution 3.0 License, which permits unrestricted use, distribution, and reproduction in any medium, provided the original work is properly cited.